

COMPARING BUILDING SURFACES' ORIENTATIONS TO OPTIMIZE SOLAR ENERGY COLLECTION

Brian A. Rock,¹ Ph.D., P.E., F.ASHRAE

ABSTRACT

Net-zero and other high performance green buildings normally do or should include optimized solar energy systems. While detailed computer-based energy simulations of buildings' energy systems are becoming near-commonplace for many projects, simple, easy-to-use data tables are beneficial earlier in the design process to help guide preliminary decisions in all projects. Practical lookup tables, and then comparison of the data they contain, are also very useful for teaching new concepts, in this case for learning about solar orientations in sunny locations.

Engineers, architects, design-build contractors, students, and other designers of green buildings can benefit through knowing, in advance, how exterior surfaces' orientations increase or decrease the total annual solar energy arriving upon those surfaces. For example, maximizing the incoming energy on a particular roof is advantageous for gathering solar energy for heat or for conversion of that sunlight to electricity, but various requirements often limit designers' choices for surfaces' orientations. This paper presents simple tables that form a tool for making initial decisions on surfaces' directions and slopes; the user can then study various effects further, such as local factors including cloudiness and shading, with detailed software. The classical solar geometry equations utilized are documented here for repeatability of the research, but are not necessary for use of this paper's tables. Practical examples are given too to help readers use the tables.

KEYWORDS

building envelopes, windows, roofs, solar geometry, solar collector, photovoltaics

1. INTRODUCTION

With global concerns about energy supply and use, optimizing the performance of buildings and increasing utilization of renewable energy are key components for improving sustainability. Sunlight arrives on buildings' windows, walls, roofs, and solar energy collectors at incidence-angles that vary with geographic location, time of day, and the day of the year. Weather, other atmospheric effects including local air pollution, and site-specific shadows reduce the delivered energy. The solar energy arriving on a surface, during a perfectly clear day—thus neglecting

1. The University of Kansas, 1530 W. 15th Street, Lawrence, KS 66045 USA, E-mail: docrock@ku.edu

atmospheric effects—would be relatively constant if that surface tracked perfectly the movement of the Earth relative to the Sun. However, more common is that the surfaces of interest are in ‘fixed’ positions, e.g., vertical walls and windows that are pointed in specific directions, roofs and skylights that are flat or sloped, and solar energy collectors that are mounted at particular angles and cardinal directions. The latter are typically installed on buildings’ roofs, and, to a lesser extent except for utility-scale systems, on ground-mounted frames. For many decades students have learned about solar effects on buildings via, for example, the various discussions presented in McGuinness et al. ([1]) and other textbooks. A now-obsolete cooling-load hand calculation method provided a table of heat gain coefficients for various exposures, but those data included mass and surface effects and were not specifically, and solely, the arriving solar energy as was sought in this project.

Designers often choose the orientations for buildings’ exteriors very early in the design process; many of those surfaces admit or use solar energy via windows, clerestories, light tubes, skylights, and solar energy arrays. A surface of interest may or may not be at the optimal orientation to the Sun to maximize the annual sunlight arriving upon it. Detailed, parametric runs of rigorous transient simulation programs such as TRNSYS (Klein [2]) are needed to determine the best positioning for a particular existing or proposed installation, but these simulations are often only performed after designs are well developed, if done at all. Various rapid online calculators are also available, e.g., Boxwell’s [3], as well as detailed models such as NREL’s SAM or PVWatts [4] for many applications; detailed models such as these use substantially the same solar-geometry equations as this study, or actual site-specific transient weather data, for their solar energy performance predictions. Some, such as F-Chart and PV F-Chart, use curve-fits developed from thousands of TRNSYS runs, for example. Simplified guidance provided earlier in the design process, via well-documented hand calculation tools such as presented in this paper, along with experience and further tempered with knowledge of the building’s local conditions, should reduce the time needed for simulations and design changes. For gauging their usefulness, the results in this paper were utilized briefly by the author in two solar energy-related courses; their students stated that the tables were very helpful in understanding the effects of solar-geometry.

Solar energy systems’ designers and installers are frequently presented with potential mounting-surfaces that are already at unchangeable directions and tilts, e.g., a choice between two or more existing or proposed roof areas, each with at least good solar access. In the earliest phases of consulting with their clients, these practitioners would also benefit from practical tables that allow making rapid initial comparisons of the tilted surfaces’ potentials. Later, solar designers will hopefully employ detailed transient simulations to refine their systems’ designs, but often they rely on simpler tools such as spreadsheets and rules-of-thumb such as ‘equivalent hours of sunshine.’

This study’s findings provide a rapid means for determining the effect of surface orientation on the total annual direct ‘clear sky’ solar energy falling upon such mentioned surfaces. While this study’s results were originally intended for initial design-purposes in North America, they should be useful as well to other locations within the range of latitudes reported for the Northern Hemisphere. These latitudes, from 20 to 60°N, covers from the southern-most Hawaiian Islands, about 20°N, to northern Canada and southern Alaska, 60°N, for example, as well as the sunnier parts of Eurasia. With care, and likely a slight reduction in accuracy as will be explained, the results should be applicable to the same latitudes in the Southern Hemisphere if the results’ north and south designations are swapped.

1.1 Prior Similar Research

Many researchers have addressed the question of optimal solar-collection positioning. For example, in their early study of this question, Kern and Harris [5] found that real local weather conditions affect the optimal collection-slope, but not too dramatically—the optimal remained near the prevailing rule-of-thumb that the surfaces' tilt angle, up from horizontal, should be equal to the local latitude. Salih and Kadim [6] studied experimentally the effect of tilt angle on fixed-position photovoltaics' (PVs') performance, and confirmed that their electrical output increased as the tilt varied from horizontal to that equal to the local latitude; they suggested a 'tilt impact factor' (TIF) for future evaluations in performance. Mondol et al. [7] performed a study of grid-connected PV arrays' orientation and slope using TRNSYS simulations. They found that performance was the same for equal east- or west-facing orientations relative to south in the Northern Hemisphere, and that the optimal slope was not horizontal. Darhmaoui and Lahjouji [8] proposed a method of finding the optimal south-facing tilted surfaces' incident energy in the Mediterranean region based on the horizontal daily global insolation, but that optimal PV orientations are dependent on their connected-utility's tariff-structures, e.g., that PV electricity sold in the late afternoon, during the utility's peak-demand period, is more valuable than that sold to the same utility in the morning. There are many case-study papers in the literature in which specific solar energy systems' collectors' slopes were studied for their particular locations, weather, and other factors; a literature search using terms optimum+tilt+angle+solar+energy+collection gives many dozens of such studies, for example.

Christensen and Barker's [9] and others' results approached closely the goal of this paper's—to provide a very rapid, direct-lookup, offline way for estimating, early in the design process, the effect of less-than-optimal orientations at various locations. Typically contour plots were developed in studies such as Christensen and Barker's, and, for example, these researchers adjusted their results with climate-dependent factors. However, the various contour plots in the literature don't quite provide what's usually desired by designers and students, for example—well-documented, very easy to use tables of values. This paper's results meet that need through clear, practical clear-sky tables for various locations' latitudes and surfaces' directions and slopes. The data for these tables were determined, too, through classical solar geometry relationships and then a custom transient simulation program; the next sections present the relationships used for this and similar papers and allow the research to be repeated or modified. *Those readers who are already very familiar with buildings' and solar geometries may wish to skip ahead to the Results and Discussion section of this paper.*

2. BUILDINGS' GEOMETRY

Buildings are most often composed of horizontal surfaces such as floors and, if so designed, flat roofs. The 'tilt' or 'slope' of these flat surfaces is 0 degrees (°) due to the most common definition that horizontal is 0°; infrequently, in the past, horizontal surfaces had been defined as at 90° by some. Walls, windows, and doors are usually vertical, thus are tilted up 90° relative to a horizontal floor. However, the surfaces that compose a building's exterior do not have to be horizontal or vertical with a common example being pitched roofs; 'pitched' means that the roofs are tilted up at a slope greater than 0°. Later in this paper, a table of common roof pitches is given for convenience.

A building's 'azimuth angle' is the direction or 'bearing' in which its main façade faces; this angle is usually defined relative to north or south. For example, if a building faces south its

azimuth angle is 180° if defined vs. north. Or it would have an azimuth angle of 0° if defined relative to south; both conventions are used. For examining the solar energy falling upon buildings, each of its surfaces' tilt and azimuth angles need to be determined. Often a goal is to maximize the solar energy arriving upon a particular surface such as a window or solar energy collector, but in other cases surfaces' orientations are selected to minimize it. An example of the latter is of windows for art galleries where natural light is preferred for viewing quality, but direct sunlight fades artwork too quickly; in these cases 'north light' is often chosen in the Northern Hemisphere.

3. SOLAR GEOMETRY

Figure 1 shows the Sun-to-surface 'solar geometry' where the plane shown is positioned flat at some location on Earth, thus the surface is defined as 'horizontal.' For the forthcoming solar geometry equations, the location's latitude (lat) on Earth is needed, but not its longitude because of the Earth's shape and rotation. An imaginary 'normal' vector (\hat{n}) is shown in Figure 1 that rises vertically (90°) out of the horizontal surface from a point defined by the intersection of the North-South and East-West cardinal directions' lines at that location.

Throughout a clear day, incoming solar radiation ('insolation') from the Sun arrives upon the horizontal surface. The Sun's 'rays,' relative to the surface, are depicted in Figure 1 as a second vector; this vector arrives from the Sun to the point of interest on the horizontal surface. The time-varying angle created between this vector of the Sun's 'direct' rays and the surface's normal vector is the 'solar zenith angle,' θ_s , as shown in Figure 1. The 'solar altitude angle,' α_s , is the angle between horizontal plane and the Sun's vector. The solar zenith and altitude angles, if added together, would usually be 90° so are related via

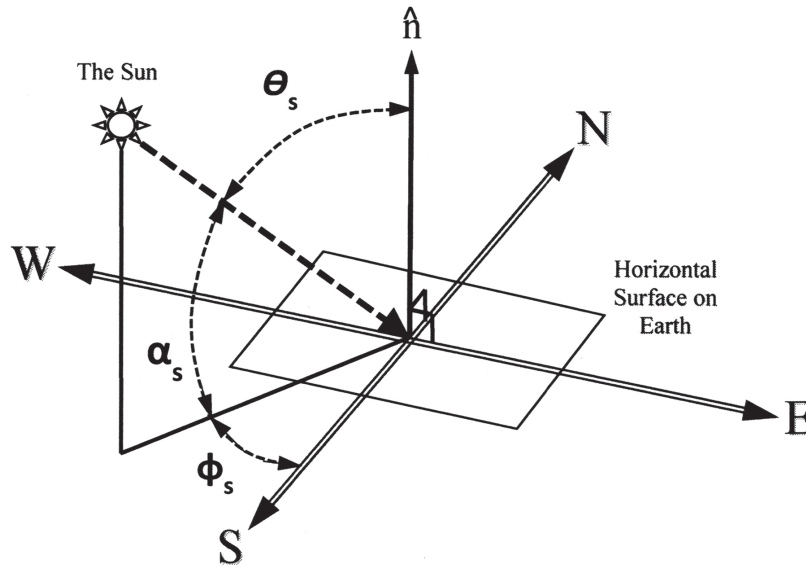
$$\theta_s = |90^\circ - \alpha_s|. \quad (1)$$

The absolute value is presented in Equation 1, unlike in most publications, because at northern latitudes on Earth between the Tropic of Cancer (about 23.45°N ; varies slowly) and the Equator (0° latitude), around solar-noon and at or near the summer solstice on about June 21st in the Northern Hemisphere, the Sun's altitude angle exceeds 90° ('goes beyond overhead'); for the Southern Hemisphere this occurs between the Tropic of Capricorn (about 23.45°S) and the Equator at or near its summer solstice, about December 21st.

Next, in defining the basic solar geometry, is to create an imaginary plane that has both the surface's normal vector (\hat{n}) and the Sun's vector within it; in Figure 1 this vertical plane would define a horizontal line as it passes through the horizontal surface's plane. The angle between this new horizontal line and true solar-south, in the Northern Hemisphere, is the 'solar azimuth angle,' ϕ_s .

The solar zenith, altitude, and azimuth angles all change continuously throughout the year. 'Solar noon,' each day, is when the solar azimuth angle is zero and the Sun is at its highest point on its 'path through the sky.' At each latitude, the largest solar altitude angle of a year will be at solar noon on the summer solstice—approximately June 21st in the Northern Hemisphere, and the smallest solar-noon altitude angle is on the winter solstice—about December 21st. At each day's sunrise and sunset on the horizontal surface, the solar altitude angle is zero, but the solar azimuth angle at sunrise and sunset varies with the particular day of the year and the local

FIGURE 1. Sun-to-horizontal surface on Earth geometry. The solar altitude angle is α_s , the solar zenith angle is θ_s , and the solar azimuth angle is ϕ_s .



latitude. On both the vernal and autumnal equinoxes—each on or near March 21st and August 21st but which equinox’s date depends on if in the Northern or Southern Hemisphere—sunrise and sunset are due east and west, respectively, for a flat, horizontal surface at any location on Earth. Note that actual sunrise and sunset times are different due to the curvature of the Earth, as well as the time-convention in use.

‘Solar time’ (st) differs from familiar ‘civil (or clock) time’ (ct) with the former defined by only the always-varying Sun-Earth geometry. The Earth rotates 360° about its axis once every 24 hours, or 15° per hour. Local solar time (st_{loc}), in hours, is defined relative to true south in the Northern Hemisphere, and varies with longitude; solar time does not utilize ‘time zones.’ At solar noon, when the Sun is at its maximum altitude angle for that day at that latitude and longitude, the local solar time is 0. Negative values of solar time indicate morning, and positive values afternoon. Solar time usually differs considerably from local civil time, but either time can be calculated from the other with design-needs’ accuracy. Only solar time was needed for this study, however. The conversion from solar time to the local ‘hour angle’ (ω_h) in degrees was needed, and is

$$\omega_h = \frac{360^\circ \cdot (st_{loc} - 12)}{24}. \quad (2)$$

The Earth’s axis of rotation is tilted about 23.45° from vertical; ‘about’ is because the Earth wobbles slightly on its axis (Bell [10]). Using an imaginary plane defined by the Earth’s annual orbital path about the Sun, the angle between the Earth’s tilt and the plane varies from about -23.45° at winter solstice to about $+23.45^\circ$ at summer solstice when in the Northern Hemisphere—reversed when in the Southern. At both the vernal and autumnal equinoxes the angle is 0° , and the day and night lengths are essentially equal on those two days of each year.

This varying angle between the Earth's axis of rotation and the orbit about the Sun is the 'sol-earth declination,' δ . To calculate the daily-average declination for each day of a generic year, instead of using the familiar Gregorian calendar, Julian day numbers (n), from 1 to 365, are utilized instead. One complete Earth orbit about the Sun requires about 365.22 days with the partial day handled through 'leap years' in civil time, but solar engineering calculations for buildings typically ignore this fractional day. One of several empirically-determined ('curve-fitted') equations for the daily-averaged value of the declination, suitable for many solar geometry predictions, is (Kreider et al. [11])

$$\delta = \sin^{-1} \left(-\sin 23.45^\circ \cdot \cos \frac{360^\circ \cdot (n + 10)}{365.25} \right). \quad (3)$$

With the declination found, and using the local latitude and current hour angle, the solar altitude angle can be determined via

$$\alpha_s = \sin^{-1} \left(\sin lat_{loc} \cdot \sin \delta + \cos lat_{loc} \cos \delta \cdot \cos \omega_h \right) \quad (4)$$

where the latitude is positive in the Northern Hemisphere. The solar azimuth angle can be found using the altitude angle from (ASHRAE [12])

$$\varphi_s = \cos^{-1} \left(\frac{\sin \alpha_s \cdot \sin lat_{loc} - \sin \delta}{\cos \alpha_s \cdot \cos lat_{loc}} \right). \quad (5)$$

Also needed for this study's computations were the sunrise (sr) and sunset (ss) hour angles ($\omega_{h, sr \text{ or } ss}$) for each day and the local latitude. Sunrise and sunset, in solar time, can be determined by setting the solar altitude angle in Equation 4 to zero and solving for the hour angle (Kreider et al. [11]). So,

$$\omega_{h, sr} = -\cos^{-1} \left(-\tan lat_{loc} \cdot \tan \delta \right), \quad (6)$$

and

$$\omega_{h, ss} = \cos^{-1} \left(-\tan lat_{loc} \cdot \tan \delta \right). \quad (7)$$

With the solar geometry to a horizontal surface on Earth defined, of next interest was varying the orientation and slope of that surface and then finding the total annual insolation falling upon it.

3.1 Sun to Tilted Surface Geometry

The surface being considered here is assumed to be on Earth and may be a solar-thermal collector, photovoltaic array, wall, window, portion of a roof, or skylight, for example. If a horizontal surface, its solar geometry is as was just described. However, surfaces are often tilted up (β_c), typically between 0 to 90° as compared to horizontal, as well as often being at a surface azimuth (φ_c) other than facing true south ($\varphi_c = 0^\circ$, in the Northern Hemisphere); such surfaces are also

known as ‘inclined planes.’ Figure 2 shows these angles as well as the surface’s solar incidence angle (θ_c) that is formed between the tilted surface’s normal vector and the Sun’s direct-beam vector. With the solar altitude (α_s) found using the previous equations for a particular latitude and hour angle, the surface’s incidence angle is (McQuiston and Parker [13])

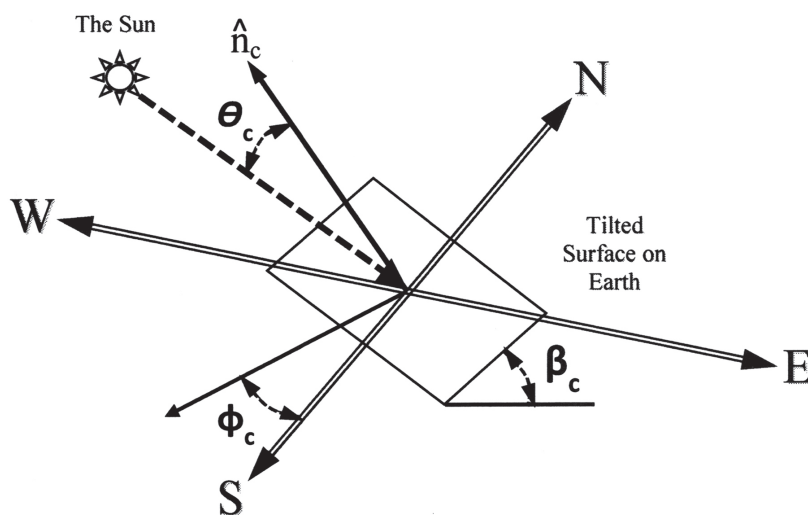
$$\theta_c = \cos^{-1} \left((\cos \alpha_s \cdot \cos \phi_c \cdot \cos \beta_c) + (\sin \alpha_s \cdot \sin \beta_c) \right). \quad (8)$$

Care is needed when using Equation 8 to check not only that the Sun has risen and not yet set, but also that the direct insolation is arriving on the front of a particular tilted surface, at that specific solar time, and not arriving on its back. This can be determined by finding the surface’s sunrise and sunset hour angles, or at that particular time by checking if the surface’s incidence angle exceeds 90° . Sunrises and sunsets, for both the horizontal plane as well as for the tilted surface, must be checked together to find the most limiting values on each day’s mornings and evenings, and for that latitude.

3.2 Solar Energy Flux on the Tilted Surface

‘Flux,’ in this usage, is the energy rate arriving on a unit area of a surface, typically in W/m^2 or $\text{BTU/h}\cdot\text{ft}^2$. The mean extraterrestrial ‘solar constant’ at Earth’s orbit, I_{sc} , is about 1373 W/m^2 ($435.2 \text{ BTU/h}\cdot\text{ft}^2$) (Duffie and Beckman [14], ASHRAE [15], and many others; this flux’s value varies slightly depending on the data source), but only a changing portion, I , reaches the surface of the Earth due to reflection off clouds, absorption, and scattering in the atmosphere. Sunlight that does arrive on a tilted surface is described in three ways: direct beam (I_D), diffuse (I_d), and reflected from other surfaces (I_r) insolation. The direct and diffuse insolation varies widely depending on length of travel through the atmosphere, weather conditions, and time of day (e.g., Erbs et al. [16]); the reflected depends on objects within line-of-sight of the surface of interest. The diffuse insolation can be as low as a few percentage of the total with a very clear

FIGURE 2. Sun-to-tilted surface geometry. The collector’s or surface’s azimuth angle is ϕ_c , its tilt up from horizontal is β_c , and the Sun-to-surface incidence angle is θ_c .



sky, to 100% on a very cloudy day. Tilting a surface up from horizontal reduces the diffuse energy flux arriving too. In routine clear-sky design, the solar flux of the diffuse component is low compared to clear-sky direct, and is thus often ignored unless detailed modeling is employed or, perhaps, a small, assumed percentage is added to the beam component or carried-through separately. In very cloudy locations, diffuse conditions may dominate and thus this study's results are of limited use there. For the general initial design purposes of this project, only the direct beam insolation was considered further. In addition to those variations, due to the eccentricity of the Earth's orbit about the Sun, the solar 'constant' varies slightly throughout the year and can be estimated to a daily-averaged value via (Kreider et al. [11])

$$I_o = I_{sc} \cdot \left(1 + 0.033 \cos \frac{360^\circ \cdot (n)}{365.25} \right). \quad (9)$$

Equation 9's variation was also included in the computer model created to generate this paper's results, and, as described later, provided data that challenges some 'conventional wisdom' on optimal orientations.

The direct solar flux arriving on a surface is reduced when that surface is not perpendicular to the Sun's rays. For each time and day, once the particular incidence angle is found between the direct-beam insolation's and a surface's normal vector, I_D on a non-perpendicular surface can be determined from (Howell et al. [17])

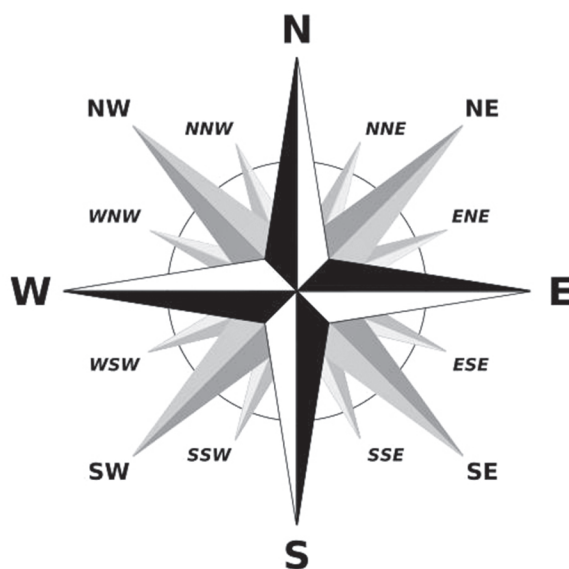
$$I_D = I_{DN} \cdot \cos \theta_c. \quad (10)$$

Again, in performing the calculations for this paper's results, care was needed to ensure that it was daytime and that sunlight was not falling upon the back of the tilted surface in each calculation time-step. The equations presented do also solve for unrealistic insolation vectors that pass through the Earth, and for surfaces that may be pointing away from the Sun at a particular time, date, and location, so, again, care is needed when performing such solar calculations.

3.3 Atmospheric Absorption and Scattering

As sunlight passes through the Earth's atmosphere, a portion of its energy is absorbed, and some photons are scattered from their direct path toward a surface. The fraction of the extraterrestrial beam solar radiation that does reach the surface is the atmosphere's transmissivity (τ_b), and has a value between 0 and 1.0. Because of the varying geometry between the Sun and a building's surface throughout the year, the path through the atmosphere varies widely in lengths, and air masses change, thus making the 'clear sky' transmissivity quite variable. In addition, the elevation of the surface, relative to sea level, also affects this transmissivity due to varying depths of the atmosphere. Different models for predicting this transient clear sky transmissivity are available; Hottel's 1976 equations and correction factors were utilized for this research (Duffie and Beckman [14]). Hottel's middle latitude correction factors for both summer and winter were used; a custom sinusoidal algorithm was created to allow these factors to vary continuously throughout the year. This latter improvement eliminated sudden changes in the correction factors as the calculations proceeded through the year for each latitude studied. Sea level was assumed; most humans live at or fairly near that elevation with about 34% of us within 100 m of it (Cohen and Small [18]).

FIGURE 3. Compass directional rose [Sebastian Brosen 2016, with GDFL permission].



3.4 Surface Azimuth Conventions

Figure 3 shows a traditional compass rose with the cardinal directions North (N), South (S), East (E), and West (W). The four major bearing subdivisions between them are shown and are Northeast (NE), Southeast (SE), Southwest (SW), and Northwest (NW). In addition, another full set of equally spaced, often less well-memorized divisions, e.g., North Northeast (NNE), are provided giving a total of 16 common directional-descriptors. With a circle being 360° , these 16 directions are 22.5° apart. Magnetic compass bearings such as N, S, E, or W are used frequently in daily civilian life in North America, e.g., ‘go west,’ instead of other directional descriptors such as degrees or ‘turn left at the corner.’ However, for solar geometry, these directions are defined relative to the true axis of rotation of the Earth, and not its magnetic poles. Over time the Earth’s poles drift significantly, so site-specific adjustments are required to convert magnetic to ‘true’ directions. A site’s local and time-dependent deviation between true and magnetic north or south, also known as the ‘magnetic declination,’ can be found easily via a web search; the U.S. government’s NOAA Geomagnetism website yields 2.3°E for the author’s location near 39°N , 95°W and date of this writing, and that it is currently moving west by about 0.1° per year.

While compass-like directions are convenient for everyday use, when modeling a surface its azimuth, in degrees, is usually needed. A problem arises that solar-design often uses, in the Northern Hemisphere, 0° azimuth to be true south, but building energy-consumption modelers, and solar-designers in the Southern Hemisphere, tend to define 0° azimuth as true north; a particular building designer may prefer either convention. To assist users, all of these directional indicators’ conventions, in 22.5° steps, are provided in this paper’s tables of results.

4. MODEL

A computer program was written to solve the preceding equations for tilted, plane surfaces in a range of northern latitudes on Earth’s surface. The program solved for the total annual

insolation arriving on fixed-position surfaces that can be at slopes from horizontal ($\beta_c = 0^\circ$) to vertical ($\beta_c = 90^\circ$), and for surface azimuths in any direction. The program currently solves in one degree increments of tilt, but only the values in ten degree increments are reported in this paper for brevity of the tables; similarly, the azimuth can be varied much more than that reported, but a 22.5° increment was desired to match the compass bearings shown in Figure 3 and as discussed previously. Internally, all angles are converted to radians as is needed by the trigonometric library functions of the programming language, and then back to degrees for the output. Separate runs of the program were performed with the latitude set from 20° to 60°N , in five degree increments, but a run for a specific latitude could be done for a particular large city such as Paris, London, or New York, for example, or a small range of latitudes for one province or country.

Each run of the program looped also on the day number of a year, from 1 to 365; a leap year-effect was not included as is common in solar design. Within each day the minute-by-minute hour angle was found, and each day looped from just-after midnight to the next midnight. Two algorithms checked if the Sun had risen or set at that location, and if it had risen or set on the surface's front side. After the surface's incident angle was found, the daily-adjusted solar constant, the atmosphere's absorption and scattering, and the cosine of the angle were used to find the solar energy flux arriving on the surface in that time step. All the time-step fluxes for the year, for while the tilted surface was illuminated by the Sun, were summed and the resulting total sent to a large digital output file.

A short, separate post-processing program read the just-mentioned output file for each latitude and then isolated the results for the desired surface tilts and azimuths. By scanning through the heat flux totals it also found the surface's angle and direction that received the maximum total annual direct solar flux. As expected, the optimal azimuth was always true solar south in the Northern Hemisphere, but the optimal slope varied slightly depending on the latitude. This second program then divided each desired slope's and azimuth's total heat flux by the maximum value and multiplied by 100% to find the percent of the optimal tilt and orientation surface's at that latitude. Because the results were intended for a wide audience, the percentages were rounded to their nearest integer values of 0 to 100%; this was also a good choice relative to the accuracy of the equations. For the same reason, small differences in the tables' data, between two similar conditions, might be ignored.

5. RESULTS AND DISCUSSION

Tables 1 through 9 present the results for northern latitudes of 20° to 60° in five degree increments; they cover most of the landmasses of North America, including Hawaii through the more-populated portions of Canada; Cuba and much of Mexico are covered as well. Although not specifically sought in this project, the values should be useable with care, e.g., for sunny locations, for similar latitudes in Eurasia, and should be reasonably accurate in the Southern Hemisphere too if the north and south designations are reversed. A separate project could produce similarly-formatted tables with data specifically for the Southern Hemisphere, and tables for the Tropics or a specific location are also possible; contact the author soon if such tables would be helpful. Another table, Table 10, is provided for 40°N and does not include the effects of Hottel's atmospheric absorption and scattering submodel, for comparison to Table 5 which does.

TABLE 1. Percent variation in total annual *direct clear sky* insolation arriving on a tilted surface as compared to the optimal surface tilt and direction at 20°N latitude.

Latitude = 20°N			Percent of Maximum Annual Insolation									
Azimuth			Collector or Surface Tilt									
True Bearing	True South	True North	(0° = Horizontal)									
			0°	10°	20°	30°	40°	50°	60°	70°	80°	90°
N	−180°	0°	95	89	79	67	54	40	29	19	11	4
NNE	−157.5°	22.5°	95	89	80	69	56	43	32	22	14	8
NE	−135°	45°	95	90	82	73	62	51	40	31	23	17
ENE	−112.5°	67.5°	95	92	86	78	69	60	51	42	34	26
E	−90°	90°	95	94	90	84	77	69	60	51	42	34
ESE	−67.5°	112.5°	95	96	94	89	83	76	67	57	47	38
SE	−45°	135°	95	98	97	94	88	80	71	61	49	38
SSE	−22.5°	157.5°	95	99	99	97	91	84	74	62	49	36
S	0°	180°	95	99	100%	98	93	85	74	62	48	35
SSW	+22.5°	202.5°	95	99	99	97	91	84	74	62	49	36
SW	+45°	225°	95	98	97	94	88	80	71	61	49	38
WSW	+67.5°	247.5°	95	96	94	89	83	76	67	57	47	38
W	+90°	270°	95	94	90	84	77	69	60	51	42	34
WNW	+112.5°	292.5°	95	92	86	78	69	60	51	42	34	26
NW	+135°	315°	95	90	82	73	62	51	40	31	23	17
NNW	+157.5°	337.5°	95	89	80	69	56	43	32	22	14	8
N	+180°	360°	95	89	79	67	54	40	29	19	11	4

Note: This data does not include diffuse or reflected insolation, nor the effects of local conditions such as weather or shading; users should consult the original source in the *Journal of Green Building* for more information about this table that is intended for use only in preliminary design.

TABLE 2. Percent variation in total annual *direct clear sky* insolation arriving on a tilted surface as compared to the optimal surface tilt and direction at 25°N latitude.

Latitude = 25°N			Percent of Maximum Annual Insolation									
Azimuth			Collector or Surface Tilt									
True Bearing	True South	True North	(0° = Horizontal)									
			0°	10°	20°	30°	40°	50°	60°	70°	80°	90°
N	−180°	0°	93	85	75	62	48	36	25	15	8	3
NNE	−157.5°	22.5°	93	86	76	64	51	38	27	18	11	7
NE	−135°	45°	93	87	79	68	57	47	37	28	21	15
ENE	−112.5°	67.5°	93	89	83	75	66	57	48	40	32	25
E	−90°	90°	93	91	88	82	75	67	59	50	42	34
ESE	−67.5°	112.5°	93	94	92	89	83	76	68	58	49	39
SE	−45°	135°	93	96	96	94	89	82	74	64	53	42
SSE	−22.5°	157.5°	93	97	99	98	94	87	78	67	54	41
S	0°	180°	93	98	100%	99	95	88	79	67	54	40
SSW	+22.5°	202.5°	93	97	99	98	94	87	78	67	54	41
SW	+45°	225°	93	96	96	94	89	82	74	64	53	42
WSW	+67.5°	247.5°	93	94	92	89	83	76	68	58	49	39
W	+90°	270°	93	91	88	82	75	67	59	50	42	34
WNW	+112.5°	292.5°	93	89	83	75	66	57	48	40	32	25
NW	+135°	315°	93	87	79	68	57	47	37	28	21	15
NNW	+157.5°	337.5°	93	86	76	64	51	38	27	18	11	7
N	+180°	360°	93	85	75	62	48	36	25	15	8	3

Note: This data does not include diffuse or reflected insolation, nor the effects of local conditions such as weather or shading; users should consult the original source in the *Journal of Green Building* for more information about this table that is intended for use only in preliminary design.

TABLE 3. Percent variation in total annual *direct clear sky* insolation arriving on a tilted surface as compared to the optimal surface tilt and direction at 30°N latitude.

Latitude = 30°N			Percent of Maximum Annual Insolation									
Azimuth			Collector or Surface Tilt									
True Bearing	True South	True North	(0° = Horizontal)									
			0°	10°	20°	30°	40°	50°	60°	70°	80°	90°
N	−180°	0°	90	81	70	56	43	31	21	12	5	2
NNE	−157.5°	22.5°	90	82	71	59	46	34	24	15	9	6
NE	−135°	45°	90	83	74	64	53	42	33	25	19	14
ENE	−112.5°	67.5°	90	86	79	71	63	54	46	38	31	24
E	−90°	90°	90	89	85	80	73	66	58	50	42	34
ESE	−67.5°	112.5°	90	92	91	87	82	76	68	59	50	41
SE	−45°	135°	90	94	95	94	90	84	76	67	56	45
SSE	−22.5°	157.5°	90	96	98	98	95	89	81	71	59	46
S	0°	180°	90	96	99	100%	97	91	83	72	60	46
SSW	+22.5°	202.5°	90	96	98	98	95	89	81	71	59	46
SW	+45°	225°	90	94	95	94	90	84	76	67	56	45
WSW	+67.5°	247.5°	90	92	91	87	82	76	68	59	50	41
W	+90°	270°	90	89	85	80	73	66	58	50	42	34
WNW	+112.5°	292.5°	90	86	79	71	63	54	46	38	31	24
NW	+135°	315°	90	83	74	64	53	42	33	25	19	14
NNW	+157.5°	337.5°	90	82	71	59	46	34	24	15	9	6
N	+180°	360°	90	81	70	56	43	31	21	12	5	2

Note: This data does not include diffuse or reflected insolation, nor the effects of local conditions such as weather or shading; users should consult the original source in the *Journal of Green Building* for more information about this table that is intended for use only in preliminary design.

TABLE 4. Percent variation in total annual *direct clear sky* insolation arriving on a tilted surface as compared to the optimal surface tilt and direction at 35°N latitude.

Latitude = 35°N			Percent of Maximum Annual Insolation									
Azimuth			Collector or Surface Tilt									
True Bearing	True South	True North	(0° = Horizontal)									
			0°	10°	20°	30°	40°	50°	60°	70°	80°	90°
N	−180°	0°	87	77	65	51	38	27	17	9	3	2
NNE	−157.5°	22.5°	87	78	66	53	41	30	20	13	8	5
NE	−135°	45°	87	80	70	59	49	39	30	23	18	13
ENE	−112.5°	67.5°	87	82	76	68	59	51	43	36	29	23
E	−90°	90°	87	86	82	77	71	64	57	49	41	34
ESE	−67.5°	112.5°	87	89	88	86	82	76	69	60	51	42
SE	−45°	135°	87	92	94	93	90	85	78	69	59	48
SSE	−22.5°	157.5°	87	94	97	98	96	92	84	75	64	51
S	0°	180°	87	94	99	100%	98	94	87	77	65	51
SSW	+22.5°	202.5°	87	94	97	98	96	92	84	75	64	51
SW	+45°	225°	87	92	94	93	90	85	78	69	59	48
WSW	+67.5°	247.5°	87	89	88	86	82	76	69	60	51	42
W	+90°	270°	87	86	82	77	71	64	57	49	41	34
WNW	+112.5°	292.5°	87	82	76	68	59	51	43	36	29	23
NW	+135°	315°	87	80	70	59	49	39	30	23	18	13
NNW	+157.5°	337.5°	87	78	66	53	41	30	20	13	8	5
N	+180°	360°	87	77	65	51	38	27	17	9	3	2

Note: This data does not include diffuse or reflected insolation, nor the effects of local conditions such as weather or shading; users should consult the original source in the *Journal of Green Building* for more information about this table that is intended for use only in preliminary design.

TABLE 5. Percent variation in total annual *direct clear sky* insolation arriving on a tilted surface as compared to the optimal surface tilt and direction at 40°N latitude.

Latitude = 40°N			Percent of Maximum Annual Insolation									
Azimuth			Collector or Surface Tilt									
True Bearing	True South	True North	(0° = Horizontal)									
			0°	10°	20°	30°	40°	50°	60°	70°	80°	90°
N	−180°	0°	84	73	60	46	34	23	13	6	3	2
NNE	−157.5°	22.5°	84	74	61	48	36	26	17	11	7	5
NE	−135°	45°	84	76	66	55	44	35	27	21	16	12
ENE	−112.5°	67.5°	84	79	72	64	56	48	41	35	28	23
E	−90°	90°	84	82	79	74	69	62	56	48	41	34
ESE	−67.5°	112.5°	84	86	86	84	80	75	69	61	53	44
SE	−45°	135°	84	89	92	92	90	86	80	72	62	51
SSE	−22.5°	157.5°	84	91	96	98	97	93	87	78	68	55
S	0°	180°	84	92	97	100%	99	96	90	81	69	56
SSW	+22.5°	202.5°	84	91	96	98	97	93	87	78	68	55
SW	+45°	225°	84	89	92	92	90	86	80	72	62	51
WSW	+67.5°	247.5°	84	86	86	84	80	75	69	61	53	44
W	+90°	270°	84	82	79	74	69	62	56	48	41	34
WNW	+112.5°	292.5°	84	79	72	64	56	48	41	35	28	23
NW	+135°	315°	84	76	66	55	44	35	27	21	16	12
NNW	+157.5°	337.5°	84	74	61	48	36	26	17	11	7	5
N	+180°	360°	84	73	60	46	34	23	13	6	3	2

Note: This data does not include diffuse or reflected insolation, nor the effects of local conditions such as weather or shading; users should consult the original source in the *Journal of Green Building* for more information about this table that is intended for use only in preliminary design.

TABLE 6. Percent variation in total annual *direct clear sky* insolation arriving on a tilted surface as compared to the optimal surface tilt and direction at 45°N latitude.

Latitude = 45°N			Percent of Maximum Annual Insolation									
Azimuth			Collector or Surface Tilt									
True Bearing	True South	True North	(0° = Horizontal)									
			0°	10°	20°	30°	40°	50°	60°	70°	80°	90°
N	−180°	0°	80	69	55	42	30	19	10	4	2	2
NNE	−157.5°	22.5°	80	70	57	44	33	22	14	9	6	5
NE	−135°	45°	80	72	62	51	41	32	25	20	16	12
ENE	−112.5°	67.5°	80	75	68	61	53	46	39	33	28	22
E	−90°	90°	80	79	76	72	66	61	54	48	41	34
ESE	−67.5°	112.5°	80	83	84	82	79	75	69	62	54	45
SE	−45°	135°	80	86	90	91	90	87	81	74	64	54
SSE	−22.5°	157.5°	80	89	94	97	97	95	89	81	71	60
S	0°	180°	80	89	96	99	100%	97	92	84	73	61
SSW	+22.5°	202.5°	80	89	94	97	97	95	89	81	71	60
SW	+45°	225°	80	86	90	91	90	87	81	74	64	54
WSW	+67.5°	247.5°	80	83	84	82	79	75	69	62	54	45
W	+90°	270°	80	79	76	72	66	61	54	48	41	34
WNW	+112.5°	292.5°	80	75	68	61	53	46	39	33	28	22
NW	+135°	315°	80	72	62	51	41	32	25	20	16	12
NNW	+157.5°	337.5°	80	70	57	44	33	22	14	9	6	5
N	+180°	360°	80	69	55	42	30	19	10	4	2	2

Note: This data does not include diffuse or reflected insolation, nor the effects of local conditions such as weather or shading; users should consult the original source in the *Journal of Green Building* for more information about this table that is intended for use only in preliminary design.

TABLE 7. Percent variation in total annual *direct clear sky* insolation arriving on a tilted surface as compared to the optimal surface tilt and direction at 50°N latitude.

Latitude = 50°N			Percent of Maximum Annual Insolation									
Azimuth			Collector or Surface Tilt									
True Bearing	True South	True North	(0° = Horizontal)									
			0°	10°	20°	30°	40°	50°	60°	70°	80°	90°
N	−180°	0°	77	65	52	38	26	16	8	4	2	2
NNE	−157.5°	22.5°	77	66	53	41	29	19	12	9	6	5
NE	−135°	45°	77	68	58	47	38	30	24	19	15	12
ENE	−112.5°	67.5°	77	72	65	57	50	44	38	33	27	22
E	−90°	90°	77	76	73	69	65	59	54	48	41	35
ESE	−67.5°	112.5°	77	80	81	80	78	74	69	63	55	47
SE	−45°	135°	77	84	88	90	90	87	82	75	67	57
SSE	−22.5°	157.5°	77	86	93	96	97	95	91	84	74	63
S	0°	180°	77	87	94	99	100%	98	94	87	77	65
SSW	+22.5°	202.5°	77	86	93	96	97	95	91	84	74	63
SW	+45°	225°	77	84	88	90	90	87	82	75	67	57
WSW	+67.5°	247.5°	77	80	81	80	78	74	69	63	55	47
W	+90°	270°	77	76	73	69	65	59	54	48	41	35
WNW	+112.5°	292.5°	77	72	65	57	50	44	38	33	27	22
NW	+135°	315°	77	68	58	47	38	30	24	19	15	12
NNW	+157.5°	337.5°	77	66	53	41	29	19	12	9	6	5
N	+180°	360°	77	65	52	38	26	16	8	4	2	2

Note: This data does not include diffuse or reflected insolation, nor the effects of local conditions such as weather or shading; users should consult the original source in the *Journal of Green Building* for more information about this table that is intended for use only in preliminary design.

TABLE 8. Percent variation in total annual *direct clear sky* insolation arriving on a tilted surface as compared to the optimal surface tilt and direction at 55°N latitude.

Latitude = 55°N			Percent of Maximum Annual Insolation									
Azimuth			Collector or Surface Tilt									
True Bearing	True South	True North	(0° = Horizontal)									
			0°	10°	20°	30°	40°	50°	60°	70°	80°	90°
N	−180°	0°	75	62	49	35	23	13	6	4	3	2
NNE	−157.5°	22.5°	75	63	50	38	26	17	11	8	6	5
NE	−135°	45°	75	66	55	44	35	28	23	19	15	12
ENE	−112.5°	67.5°	75	69	62	55	48	43	37	32	28	23
E	−90°	90°	75	74	71	67	63	59	54	48	42	36
ESE	−67.5°	112.5°	75	78	79	79	77	74	70	64	56	48
SE	−45°	135°	75	82	86	89	89	87	83	77	69	59
SSE	−22.5°	157.5°	75	84	91	96	97	96	92	86	77	66
S	0°	180°	75	85	93	98	100%	99	95	89	79	68
SSW	+22.5°	202.5°	75	84	91	96	97	96	92	86	77	66
SW	+45°	225°	75	82	86	89	89	87	83	77	69	59
WSW	+67.5°	247.5°	75	78	79	79	77	74	70	64	56	48
W	+90°	270°	75	74	71	67	63	59	54	48	42	36
WNW	+112.5°	292.5°	75	69	62	55	48	43	37	32	28	23
NW	+135°	315°	75	66	55	44	35	28	23	19	15	12
NNW	+157.5°	337.5°	75	63	50	38	26	17	11	8	6	5
N	+180°	360°	75	62	49	35	23	13	6	4	3	2

Note: This data does not include diffuse or reflected insolation, nor the effects of local conditions such as weather or shading; users should consult the original source in the *Journal of Green Building* for more information about this table that is intended for use only in preliminary design.

TABLE 9. Percent variation in total annual *direct clear sky* insolation arriving on a tilted surface as compared to the optimal surface tilt and direction at 60°N latitude.

Latitude = 60°N			Percent of Maximum Annual Insolation									
Azimuth			Collector or Surface Tilt									
True Bearing	True South	True North	(0° = Horizontal)									
			0°	10°	20°	30°	40°	50°	60°	70°	80°	90°
N	−180°	0°	73	60	46	32	20	11	6	4	3	2
NNE	−157.5°	22.5°	73	61	48	35	23	15	11	9	7	5
NE	−135°	45°	73	63	53	42	33	27	23	19	16	13
ENE	−112.5°	67.5°	73	67	60	53	47	42	38	33	29	24
E	−90°	90°	73	72	69	66	62	59	54	49	43	37
ESE	−67.5°	112.5°	73	76	78	78	77	74	70	65	58	50
SE	−45°	135°	73	80	85	88	89	88	84	78	71	61
SSE	−22.5°	157.5°	73	83	90	95	97	96	93	87	79	68
S	0°	180°	73	83	92	97	100%	99	96	90	82	71
SSW	+22.5°	202.5°	73	83	90	95	97	96	93	87	79	68
SW	+45°	225°	73	80	85	88	89	88	84	78	71	61
WSW	+67.5°	247.5°	73	76	78	78	77	74	70	65	58	50
W	+90°	270°	73	72	69	66	62	59	54	49	43	37
WNW	+112.5°	292.5°	73	67	60	53	47	42	38	33	29	24
NW	+135°	315°	73	63	53	42	33	27	23	19	16	13
NNW	+157.5°	337.5°	73	61	48	35	23	15	11	9	7	5
N	+180°	360°	73	60	46	32	20	11	6	4	3	2

Note: This data does not include diffuse or reflected insolation, nor the effects of local conditions such as weather or shading; users should consult the original source in the *Journal of Green Building* for more information about this table that is intended for use only in preliminary design.

TABLE 10. *Without atmospheric absorption and scattering, percent variation in total annual direct clear sky insolation arriving on a tilted surface as compared to the optimal surface tilt and direction at 40°N latitude. This table is for comparison-purposes only, to Table 5.*

Latitude = 40°N			Percent of Maximum Annual Insolation									
Azimuth			Collector or Surface Tilt									
True Bearing	True South	True North	(0° = Horizontal)									
			0°	10°	20°	30°	40°	50°	60°	70°	80°	90°
N	−180°	0°	80	68	56	44	33	24	17	11	7	6
NNE	−157.5°	22.5°	80	69	58	46	37	28	21	16	13	11
NE	−135°	45°	80	72	64	55	48	41	35	31	27	23
ENE	−112.5°	67.5°	80	75	71	66	62	57	52	48	43	37
E	−90°	90°	80	79	79	77	75	72	68	63	57	51
ESE	−67.5°	112.5°	80	83	85	87	86	84	80	75	68	60
SE	−45°	135°	80	86	91	93	94	92	88	82	74	64
SSE	−22.5°	157.5°	80	88	94	98	98	97	92	85	76	65
S	0°	180°	80	89	95	99	100	98	93	86	76	64
SSW	+22.5°	202.5°	80	88	94	98	98	97	92	85	76	65
SW	+45°	225°	80	86	91	93	94	92	88	82	74	64
WSW	+67.5°	247.5°	80	83	85	87	86	84	80	75	68	60
W	+90°	270°	80	79	79	77	75	72	68	63	57	51
WNW	+112.5°	292.5°	80	75	71	66	62	57	52	48	43	37
NW	+135°	315°	80	72	64	55	48	41	35	31	27	23
NNW	+157.5°	337.5°	80	69	58	46	37	28	21	16	13	11
N	+180°	360°	80	68	56	44	33	24	17	11	7	6

Note: This table is not intended for any design use; it is provided only for comparison to another table. This data does not include diffuse or reflected insolation, nor the effects of local conditions such as weather or shading; users should consult the original source in the *Journal of Green Building* for more information about this table.

5.1 Optimal Azimuths and Tilts

Tables 1 to 9 show that the optimal surface azimuth, for maximizing arriving beam solar energy over a full year, at each latitude in the Northern Hemisphere, is true-south, as was expected. The best tilts varied from equal to the latitude to something less. The developed program calculated results for one-degree increments in surface tilt instead of just the ten degree increments in tilts reported in the summary tables; ten degree increments' data were chosen to make the tables of practical size—interpolation between the data and tables may be required by users of the tables. However, the post-processing program scanned all the one-degree tilts' results and found that the optimal slopes varied from equal-to-latitude for the southern-most, slightly less than latitude for the moderate, and noticeably less for the northern-most latitudes. The optimal values of slope found for 20° to 60° latitudes, in 5° increments of latitude, were 18°, 22°, 26°, 30°, 33°, 37°, 40°, 42°, and 44° respectively. The daily variation in solar constant, Equation 9, was the second-to-last relationship added to the computational model and its inclusion increased the deviation from equal-to-latitude rule-of-thumb slightly. The last submodel added was Hottel's path-dependent atmospheric absorption and scattering; it increased the deviation at higher latitudes even more. Table 10 shows the results for 40°N without the absorption and scattering, and shows that the optimal tilt is equal to latitude, as widely reported in prior research or assumed elsewhere. Consultant Landau [18], in a webpage, presents comparable optimal-tilt results that are less than equal to the local latitude; some of his stated methods appear similar to those used here but others couldn't be determined from his webpage. This current paper's methods are fully-referenced, the results repeatable, and are publicly available via this paper.

As just mentioned, this project's findings on optimal tilts vary from others' that state the optimal is always equal to latitude; despite being a small deviation in maximum arriving energy, percentage-wise as shown in the tables, more study is recommended. The current results reflect that the Earth's orbit is eccentric—for example, at its summer solstice, the Northern Hemisphere is slightly farther from the Sun than for the Southern Hemisphere at its summer solstice; the predicted optimal slopes for latitudes in the Southern Hemisphere may vary from those in the Northern but were not studied in this project. The predicted deviation of fixed-position, annual optimal tilt may also reflect that the Earth is not a perfect sphere—it is a bit wider around the Equator due to its rotation and because the Earth is largely not a solid. In the early morning and late afternoon hours, sunlight has longer paths to travel through the atmosphere so absorbing and scattering of the direct-beam insolation is much higher than during the midday hours according to Hottel's relationship, for example; surfaces with lower tilts would therefore receive more cosine-adjusted total solar flux, summed over each day, if all other factors were held constant. Also possibly affecting this paper's deviation from prior findings is that this project examined solar energy arriving on tilted surfaces only; building- and system-effects, especially for those systems for seasonal use only such as for space heating in the winter, would influence the optimal collector slopes. Further study of this variation in optimal slope could be beneficial for improving the performance of building energy models and systems.

5.2 Variations with Other Orientations

The tables confirm other expectations, e.g., that mounted-flat surfaces' collection-potential does not depend on surface azimuth because they are horizontal, and that the potential is significantly lower than optimal for many tilt-angles in most of the latitudes examined. Thus the results confirm that horizontal surfaces are less-than-optimal from a maximum solar collection

performance point-of-view. However, the results show that the farther to the south the building's site is located in the Northern Hemisphere, the better the solar potential for horizontally-mounted skylights and collectors; at 20°N flat surfaces receive about 95% of the optimal, but this decreases to 84% at 40°N and 73% at 60°N. Vertical, south-facing windows and other surfaces are the opposite, at 35%, 56%, and 71% for those three latitudes, respectively, because of the smaller midday Sun-to-surface incidence angles when the site is farther north. This latter combination—good performance-potential for vertical, south-facing surfaces in the far north—is confirmed via, for example, the convention of mounting transpired solar collectors on southern exterior walls for preheating ventilation air in some buildings in the far north (e.g., Kutscher et al. [20]).

Another interesting observation of the results is that for subtropic latitudes of the Northern Hemisphere, the annual total direct solar energy arriving on a vertical, true-south facing surface is slightly less than if it were turned just slightly east or west. For example, for 20°N, Table 1 shows that the south-facing vertical surface receives 35% of the maximum, but 38% for that vertical surface if turned east or west 45°. If not due to a limitation of the equations, this is likely because during the longest days of the year, close to summer solstice, the 'noon sun' is not just directly overhead, but actually slightly north of overhead thus sunlight does not shine on the front of the vertical, south-facing surface in those hours. Also, just north of about 23.45°N latitude, around solar noon and at or near the summer solstice, the cosine-effect on the direct insolation makes the direct flux on the front of the vertical surface near zero. This effect is reduced, and then eliminated, the farther north the site's latitude is from 23.45°N, or conversely for the Southern Hemisphere.

The results also confirm that when the surface is positioned at the optimal slope for its latitude, the total annual direct insolation on the tilted surface does not decrease greatly when turned slightly east or west of south—the maximum reduction is only 3% for even being $\pm 22.5^\circ$ off true south in the northern-most reported latitude; for the southern-most of the tables there is even less depreciation. In the past, when photovoltaics' module prices were very high, placing an array in the optimal direction was considered crucial; with recent years' dramatic reductions in the per-watt prices of mono- and polycrystalline PV, slightly suboptimal array orientations can easily be overcome through use of slightly more, now much lower cost modules. Utilizing accurate two-axis trackers would, of course, achieve the best results, but fixed-mount arrays for solar-thermal as well as solar-electric systems on buildings are usually employed instead due to their cost-effectiveness, ease of installation, strength, reduced maintenance needs, and appearance.

5.3 Roof Slopes

Table 11 presents, for convenience, the equivalent roof slopes in degrees for popular roof-pitch descriptors that are rise vs. run, e.g., a '4 in 12' or '4/12' roof pitch is 18.4°. In North America, small-buildings' roofs are often steeper the farther north the location to enhance rain and snow shedding. However, 'flat' roofs are used on most large buildings everywhere in North America for economic as well as practical reasons. Flat roofs do generally have very slight, multi-directional slopes to encourage rainwater- and snowmelt-drainage, but these slopes are normally very small and thus neglected in solar energy predictions.

A '4 in 12' roof pitch is very popular in much of North America except in the snowiest regions, especially when utilizing pre-manufactured wooden roof trusses. If such a 18.4° sloped-roof were to face true south, double-interpolating between the two closest tables as well

TABLE 11. Equivalent surface tilt or slope, in degrees, for popular rise vs. run roof pitches.

Roof Pitch	Tilt or Slope
2-in-12 (2/12)	9.5°
4-in-12 (4/12)	18.4°
6-in-12 (6/12)	26.6°
8-in-12 (8/12)	33.7°
10-in-12 (10/12)	39.8°
12-in-12 (12/12)	45°

as between tilts for each shows that in Orlando, FL (28.54°N) that surface should receive about 99% of the optimal slope's annual total direct-beam insolation; in Atlanta, GA (33.75°N) about 98%; in Washington, D.C. (38.91°N) about 97%; and in Boston, MA (42.36°N) about 96%. In Calgary, AB (51.05°N), the most northerly of these mentioned locations, a south-facing 4 in 12 roof would still receive about 93% of the optimal total. These values show that even a modestly-sloped surface would receive a very high proportion of the optimal annual direct insolation if its azimuth is toward or near true south in the Northern Hemisphere, except likely in the very far northern latitudes beyond the range of this study. The applications in the next section demonstrate the effect of more significant deviations from the optimal tilt and azimuth.

6. EXAMPLE APPLICATIONS

The following examples are from actual projects near 40°N latitude. For simplicity, the compass directions stated include already the effect of the local magnetic deviation.

Horizontal installation of PV: A proposed building with a flat roof was to have a demonstration PV array. However, the building's designer or client did not want the array to be visible from street-level, so the choice was made to mount the modules horizontally. From Table 5 the total annual direct insolation upon the array, not including reflections or shading, would be about 84% of optimal if the array were facing true south and tilted up optimally. To gain similar performance to the best orientation, not including diffuse insolation as well as system, site, or weather effects, the horizontally-mounted array needed to be increased in size by about $((1/0.84) - 1) \times 100\% = 19\%$.

West-facing solar-thermal collectors: An existing single-family house has a large roof area tilted at about 30°, however the house and that portion of its roof faces due-west. From Table 5, if the building were instead pointed due-south the maximum annual direct insolation would fall upon solar collectors tilted at 30°. However, also from Table 5, with the 30° roof actually facing west, the collection-potential is 74% of optimal, rounded to the nearest whole number, so was reduced by 26% by the original design-decision to orient the building and that portion of its roof west instead of south.

Deciding between two roof sections of the same azimuth, but different slopes: An existing building's multifaceted roof is oriented about 33° west of south, and has available two large roof-sections at that azimuth with different slopes: 20° and 45°. Linearly-interpolating the values in Table 5, and then rounding, yield that the $\beta = 20^\circ$ and $\beta = 45^\circ$ roof sections receive about 94%

and 92%, respectively, of an optimal $\varphi = 0^\circ$ and $\beta = 30^\circ$ surface's annual total incident solar radiation. With only about a 2% difference between the two, either would require about the same area of solar collectors or glazings to receive the same annual-average direct, clear-sky solar energy. However, if seasonally-optimized collection is desired, the steeper-sloped portion should be selected for winter-optimization, e.g., for solar-thermal space heating, and the shallower for summer, e.g., for summer-peaking photovoltaics as described by others in the literature, and demonstrated through actual installations.

The preceding examples show how the tables can be used to provide insight during the preliminary design phase of a solar energy project in a sunny climate, or for academic study of or research on similar. For more precise results, the preliminary findings should then be examined via a detailed computer-based simulation that includes local effects such as the site-specific weather. New users of the tables presented here are encouraged to read this entire paper to understand the data's limitations.

7. CONCLUSIONS AND RECOMMENDATIONS

This paper's results are a series of new tables, 1 through 9, and their descriptive captions intended, together, as a tangible and practical learning and early-stage design tool, e.g., for the rapid-comparison of tilted surfaces' directions on total annual incident direct clear-sky solar energy in sunny to mostly-sunny locations. It was observed before completion of this project that the need for such tables existed for at least quick, initial observations of tilted surfaces' solar energy arrival on buildings' windows and for solar energy-gathering equipment such as solar-thermal collectors and photovoltaic modules. The tables' incident-energy potentials, expressed in easily-understood percentages of the maximum possible, should also be helpful for solar contractors, for students learning about the Sun's effects on buildings' surfaces, and for educating clients about optimal surfaces' orientations and the consequences of other tilts and directions. In addition to the goal of helping to select surface orientations to maximize insolation, the tables may also be used for the opposite purpose of comparing directions and tilts that minimize total annual direct insolation, e.g., for art installations that are faded by sunlight. The tables may also be useful for those characterizing relative degradation of roofing, siding, or exterior paint. While found for North American latitudes, the results should be applicable to the same latitudes in Europe and Asia with clearer-sky weather. Data for more-specific or other latitudes and surface orientations could be generated using the two computer programs developed in this study. Users of this paper's tables need to be aware that the tables' data do not include surface effects such as directionally-dependant absorptance, dirt or snow accumulation, building-mass, system-effects, nor local influences such as other weather effects, smog, shading, or existence of near-by reflective surfaces. Also, the compass-like directions shown in the tables should be adjusted with a location's magnetic deviation as is described in the body of this paper and elsewhere.

Further research is needed to develop similar tables for optimal single-season angles. These tables would be useful, for example, in selecting grid-connected PV arrays' positioning where utilities' tariff-rates vary on if the utilities' demand-curves are summer- or winter-peaking, or for seasonal-use of buildings. Additionally, further study is needed to examine this project's results showing that optimal surface slopes, for maximizing annual incident beam solar energy, are slightly less than that equal to the local latitude for the more-northerly sites in the Northern Hemisphere; these variations may be due to natural variations in the Earth and its orbit, or the effects of the atmosphere at differing solar incidence angles, for example. Additionally, tables for

fairly cloudy or smoggy locations, where diffuse solar radiation may dominate design-decisions, are needed.

8. ACKNOWLEDGMENTS

The author expresses his gratitude to his former solar energy professors, Thomas S. Dean (deceased), Gary C. Vliet, and Jan F. Kreider, as well as his former colleagues at SERI/NREL. This work was supported by Rock Consulting Engineers and the University of Kansas, both of or near Lawrence, KS.

9. NOMENCLATURE

ct = civil time, hours

I = incident or incoming solar radiation, a.k.a. insolation, W/m^2 ($\text{BTU/h}\cdot\text{ft}^2$)

lat = latitude on Earth, 0 to 90°

n = Julian day number, 1 to 365

\hat{n} = unit normal vector

N = north

st = solar time, -12 to $+12$ hours

Greek

α = solar altitude angle

β = tilt or slope, 0 to 90°

δ = solar declination, -23.45 to $+23.45^\circ$

θ = Sun-to-surface angle, zenith (θ_z) or incident (θ_c)

φ = azimuth angle of the Sun (φ_s), surface (φ_c), or building; 0° = true south

ω = solar hour angle, -3.14159 to $+3.14159$ radians

Subscripts

c = collector or surface, or Sun to tilted surface

D = direct

d = diffuse

DN = direct normal

h = hour

loc = local

o = extraterrestrial

r = reflected

s = solar or Sun, or Sun to horizontal surface

sc = solar constant

sr = sunrise

ss = sunset

T = terrestrial

10. REFERENCES

1. McGuinness, W., B. Stein, J. Reynolds, J. Stein, W. Grondzik, or A. Kwok, and possibly other authors of the many editions of the architectural textbook *Mechanical and Electrical Equipment for Buildings*. The current edition is the 13th, October (2019), John Wiley & Sons, NY.
2. Klein, S. A. (2017). *TRNSYS 18: A Transient System Simulation Program*. Solar Energy Laboratory, University of Wisconsin, Madison, USA. sel.me.wisc.edu/trnsys
3. Boxwell, M. (2017). "The Solar Electricity Handbook," solarelectricityhandbook.com, accessed 16 January 2017.
4. NREL (2017). *System Advisor Model (SAM)*, software for detailed evaluation of specific renewable energy systems, and *PVWatts*, and online calculator. The National Renewable Energy Laboratory (of the U.S. Department of Energy), Golden, Colorado, USA. sam.nrel.gov and pvwatts.nrel.gov.
5. Kern, J., and I. Harris, May (1975). "On the Optimum Tilt of a Solar Collector," *Journal of Solar Energy*, vol. 17, pp. 97–102.
6. Salih, M. S., and L. A. Kadim (May 2014). "Effect of Tilt Angle Orientation on Photovoltaic Module Performance," *ISECO Journal of Science and Technology*, vol. 10, no. 14, pp. 19–25.
7. Mondol, J. D., Y. G. Yohanis, and B. Norton (2007). "The Impact of Array Inclination and Orientation on the Performance of a Grid-Connected Photovoltaic System," *Renewal Energy journal*, Elsevier, vol. 32, pp. 118–140.
8. Darhmaoui, H., and D. Lahjouji (2013). "Latitude Based Model for Tilt Angle Optimization for Solar Collectors in the Mediterranean Region," *Energy Procedia*, vol. 42, pp. 426–435. Proceedings of the Mediterranean Green Energy Forum 2013.
9. Christensen, C. B., and G. M. Barker (2001). "Effects of Tilt and Azimuth on Annual Incident Solar Radiation for United States Locations," *Proceedings of Solar Forum 2001*, April 21–25, Washington, D.C., pp. 225–232.
10. Bell, T. E. (Spring 2016). "Wandering Pole, Wobbling Grid," *The Bent of Tau Beta Pi*, Vol. 107, no. 2, pp. 14–18.
11. Kreider, J. F., P. S. Curtiss, and A. Rabl (2002). *Heating and Cooling of Buildings, Second Edition*. McGraw-Hill, New York.
12. ASHRAE (1992). *ASHRAE Cooling and Heating Load Calculation Manual, Second Edition*. ASHRAE, Inc., Atlanta, Georgia.
13. McQuiston, F. C., and J. D. Parker (1994). *Heating, Ventilating, and Air Conditioning, Fourth Edition*. John Wiley & Sons, New York.
14. Duffie, J. A., and W. A. Beckman (2013). *Solar Engineering of Thermal Processes, Fourth Edition*. John Wiley & Sons, New York.
15. ASHRAE (1997). Fundamentals volume of the *ASHRAE Handbook*. ASHRAE, Inc., Atlanta, Georgia.
16. Erbs, D. G., S. A. Klein, and J. A. Duffie (1982). "Estimation of the Diffuse Radiation Fraction for Hourly, Daily and Monthly-Average Global Radiation," *Solar Energy*, vol. 28, pp. 293–302.
17. Howell, J. R., R. B. Bannerot, and G. C. Vliet (1982). *Solar-Thermal Energy Systems: Analysis and Design*. McGraw-Hill, New York.
18. Cohen, J. E., and C. Small (1998). "Hypsographic demography: The distribution of human population by altitude," *Proceedings of the National Academy of Sciences in the United States*, November 24, 1998, vol. 95, no. 24, pp. 14009–14014.
19. Landau, C. R. (11 November 2015). "Optimum Tilt of Solar Panels," an Internet white paper offering consulting services. www.solarpaneltilt.com, last accessed 27 December 2018.
20. Kutscher, C. F., C. B. Christensen, and G. M. Barker (August 1993). "Unglazed Transpired Solar Collectors: Heat Loss Theory," *Journal of Solar Energy Engineering*, vol. 115, pp. 182–188.